

ViFi-ReID: A Two-Stream Vision-WiFi Multimodal Approach for Person Re-identification

Chen Mao, Chong Tan, *Member, IEEE*, Jingqi Hu, and Min Zheng

Abstract—Person re-identification(ReID), as a crucial technology in the field of security, plays a vital role in safety inspections, personnel counting, and more. Most current ReID approaches primarily extract features from images, which are easily affected by objective conditions such as clothing changes and occlusions. In addition to cameras, we leverage widely available routers as sensing devices by capturing gait information from pedestrians through the Channel State Information (CSI) in WiFi signals and contribute a multimodal dataset. We employ a two-stream network to separately process video understanding and signal analysis tasks, and conduct multi-modal fusion and contrastive learning on pedestrian video and WiFi data. Extensive experiments in real-world scenarios demonstrate that our method effectively uncovers the correlations between heterogeneous data, bridges the gap between visual and signal modalities, significantly expands the sensing range, and improves ReID accuracy across multiple sensors.

Index Terms—Person re-identification, WiFi CSI signal, Two-stream network, Feature Fusion

I. INTRODUCTION

Person ReID is a crucial task in the field of security surveillance. Due to limitations in camera resolution and shooting angles, obtaining high-quality facial images for face recognition is often not feasible. Therefore, ReID emerges as a significant technology for the identification of individuals or objects in such scenarios. In recent years, the task has attracted widespread attention from both the academic and industrial communities due to its potentially important applications in large-scale surveillance networks, demonstrating significant research impact and practical value.

In current mainstream vision-based ReID methods [1]–[7], RGB images are susceptible to negative impacts from lighting, obstructions, and pedestrian clothing, and the deployment range of cameras is limited. Some multimodal ReID methods [8]–[11], utilizing infrared cameras, LiDAR, and other devices, can mitigate the issue of low recognition accuracy at night but lead to a significant cost burden. Some methods [12]–[23] based on WiFi signals offer a new approach to pattern recognition. Routers, as widely available sensing sensors, are distributed in places where cameras are not commonly installed. In wireless communication, the impact of the physical environment on WiFi signals can be described through CSI. As pedestrians pass by, the signals emitted by the transmitter scatter and reflect off the human body, and the receiver captures the signals over a period of time. This information



Fig. 1: A pair of WiFi transceivers and a camera are used to identify the person

implicitly describes the pedestrian’s gait and posture information, enabling differentiation between individuals based on their unique characteristics.

Both pedestrian videos and WiFi temporal signals can reflect pedestrian gait information. Videos additionally include RGB color and pedestrian motion, while WiFi adds spatial positioning information, indicating that there is both correlation and complementarity between the two modalities. We propose a multimodal approach based on both vision and WiFi signals, which can utilize existing cameras and routers in the real world to accomplish the task of person ReID. In practical scenarios, if some areas have only cameras, only routers, or both, then it is possible to link this person’s ID across different modal scenes. This ensures the continuity of ReID across different modalities, rather than multiple isolated systems. The method works in both single-modal and multimodal scenarios, bridging the gap between heterogeneous data and expanding the coverage of ReID tasks.

For the WiFi signal module, we encode the WiFi signals within fixed time units and add temporal tokens to the raw encoding to capture the temporal information in the signals. For the video sequence module, we employ independent spatial and temporal encoder [24], [25] to extract pedestrian motion features from the video. And we use merged attention mechanism to connect the feature vectors of the two modalities. Representation learning and metric learning are applied to the network’s final predictions and cascaded feature layers, generating a more comprehensive pedestrian feature representation. Additionally, to explore the relationship between the two modalities, we design a loss function based on contrastive learning and hard example mining to achieve cross-modal matching. In addition, We introduce a challenging

vision-WiFi person ReID dataset, comprising both pedestrian videos and WiFi data, which provides data support for future related research.

II. DATASET

We contribute a multimodal person ReID and retrieval dataset named ViFi-Indoors, based on a real indoor environment. The ViFi-Indoors not only contains video sequence data of pedestrians but also synchronously collects WiFi signal data from routers in the scene. Figure 2 shows some visual examples of video and corresponding WiFi signals from the dataset.

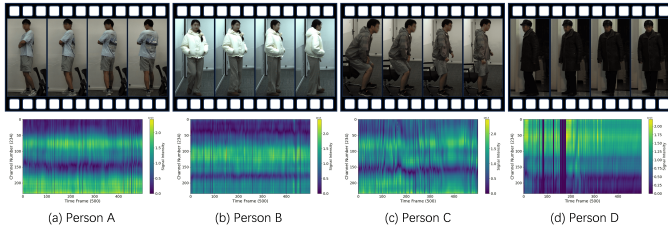


Fig. 2: Example of one video clip of a sample and the corresponding matrix of WiFi CSI data frame.

Video sequence: Our dataset contains three different real indoor scenes. To ensure the authenticity of data collection, we film a diverse range of persons including men, women, elderly, and children. The subjects being filmed are in challenging scenarios, including wearing masks, partial body obstructions, multiple persons wearing similar clothing, and a single person wearing different clothes in different scenes. Ultimately, the vision data comprises 1380 video sequences from 20 persons, totaling 34,500 frames.

WiFi signal: We use 234 subcarriers and employ a single antenna for transmission and four antennas for reception, forming a 1×4 MIMO matrix. The WiFi signals are transmitted at a frequency of 100 times per second. To maintain synchronization with the video, we concurrently collect WiFi signals during video recording, setting 5 seconds as a WiFi signal unit. Therefore, the dimension of the WiFi signal unit

is $500 \times 4 \times 234$. Corresponding to the video collection, our WiFi data also includes 1380 signal units from 20 persons.

III. PROPOSED METHOD

A. Video Feature Extraction

The architectural diagram of the neural network model is shown in Figure 3. Drawing from the core principles of the ViViT video classification model based on the Transformer architecture [25], we construct two separate Transformer encoders. The spatial encoder, serving as the first part, solely models the interactions between tokens extracted from identical temporal indices. After undergoing L_s layers of spatial Transformers, we acquire a spatial feature representation for each frame, $h_i \in \mathbb{R}^{d_s}$. These frame-level features h_i are then amalgamated into $H \in \mathbb{R}^{n_t \times d}$, which is subsequently input into a temporal encoder comprised of L_t Transformer layers. This temporal encoder is tasked with modeling interactions between tokens from disparate temporal indices, thereby capturing the dynamic correlations between various frames.

B. WiFi Feature Extraction

Modern WiFi devices adhere to the IEEE 802.11n/ac standards, utilizing Orthogonal Frequency-Division Multiplexing (OFDM) at the physical layer, which allows the use of multiple transmitting and receiving antennas to achieve Multiple Input Multiple Output (MIMO) communication. WiFi signals transmitted between routers undergo changes influenced by the physical environment. The CSI in WiFi reveals the fine-grained characteristics of delay, amplitude attenuation, and multipath phase shift effects on each communication subcarrier.

To extract features from sequential WiFi signals, we propose a straightforward and practical method for representing feature vectors. As shown in Figure 4, drawing inspiration from the natural language processing method BERT [26], we introduce a method named WiFormer for vector representation of WiFi signals. Given that WiFi signals are naturally composed of digits during transmission, we take the absolute value of the signal's complex data and normalize it. Then, on the base

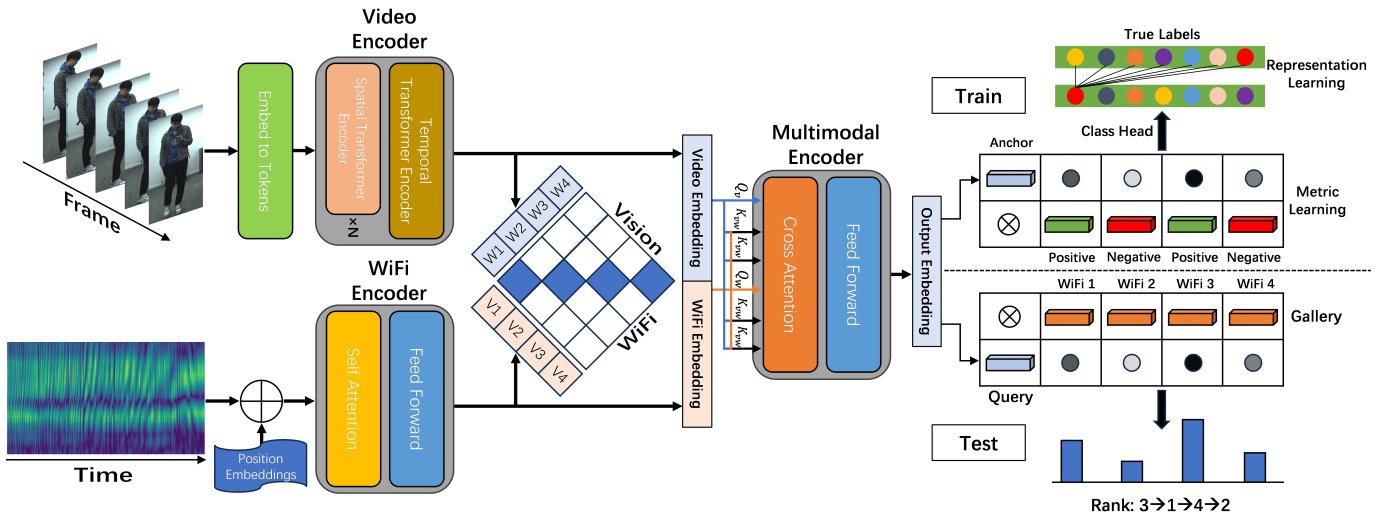


Fig. 3: The overall architecture diagram of ViFi-ReID.

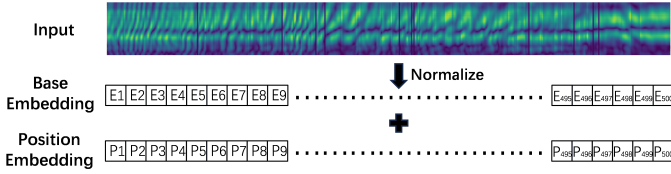


Fig. 4: WiFi Data Preprocessing in WiFormer.

embedding of the corresponding time frame, we add learnable position embeddings to denote the location of each moment in a CSI sequence. The processed data is fed into multiple layers of bidirectional Transformer Encoders for analysis, utilizing self-attention mechanisms to address the long-distance dependencies of sequential signals.

Cross-modal fusion facilitates the complementarity of various heterogeneous information. Both video and WiFi implicitly contain information about pedestrian walking gait, and video sequences contain additional color information, while WiFi signals provide extra spatial perception information. The goal of the fusion network is to process and correlate information from multiple modalities to achieve more effective complementarity. We employ merged attention [27] to fuse video and WiFi embeddings. The multimodal fuse module is composed of multi-head cross-attention and multi layers of transformer encoder blocks. The features from both modalities, extracted from the previous stage’s two-stream network of video and WiFi, are concatenated and fed into the feature fusion network and adaptively fused through the cross-modal attention mechanism.

C. Representation and Metric Learning

We place the large margin cosine loss [29] behind the classification head of the model and SoftTriple [30] at the feature output layer, aiming to enhance the representation capability of the model by maximizing intra-class similarity and inter-class dissimilarity and effectively learn the fine-grained structure of categories within the feature space.

$$L_{LMCL} = -\frac{1}{N} \sum_{i=1}^N \log \frac{e^{s(\cos(\theta_{y_i})-m)}}{e^{s(\cos(\theta_{y_i})-m)} + \sum_{j \neq y_i} e^{s \cos(\theta_j)}} \quad (1)$$

where N is the batch size, θ_{y_i} is the angle between the feature vector of the correct class and the weight vector, m is the introduced margin, and s is the scaling factor.

$$L_{SoftTriple} = \frac{1}{N} \sum_{i=1}^N \log \frac{1 + \sum_{j=1}^C \sum_{k=1}^K \exp(-\sigma(d(x_i, c_{jk}) - \delta))}{\exp(\lambda) + \sum_{j \neq y_i} \sum_{k=1}^K \exp(-\sigma d(x_i, c_{jk}))} \quad (2)$$

where N is the batch size, C is the number of categories, K is the number of centers per category, $d(x_i, c_{jk})$ is the distance between sample x_i and center c_{jk} of category j , σ is the scaling parameter, and δ and λ are parameters controlling the degree of separation between and within categories, respectively.

D. Contrastive Learning for Multimodality

We explore the relationships between vision and signals through contrastive learning, enabling mutual retrieval across different modalities. Unlike CLIP [31], we apply a supervised contrastive learning method [32] to the multimodal matching task of vision and WiFi, learning feature representations by minimizing the distance between matching vision-WiFi pairs and maximizing the distance between non-matching pairs. This approach aims to enhance the aggregation of matching pairs in the feature space and strengthen the model’s ability to differentiate between non-matching pairs. The formula is as follows:

$$\mathcal{L}_{w2v} = -\frac{1}{N} \sum_{i=1}^N \frac{1}{|P(i)|} \sum_{p \in P(i)} \log \frac{\exp(s(w_i, v_p)/\tau)}{\sum_{j=1}^N \exp(s(w_i, v_j)/\tau)} \quad (3)$$

$$\mathcal{L}_{sup} = \mathcal{L}_{w2v} + \mathcal{L}_{v2w} \quad (4)$$

where N is the size of a batch, P_i is the set of indices of all positive samples in the batch for the i -th sample. $s(w_i, v_j)$ represents the similarity between the WiFi feature and the vision feature, which is the dot product of the embeddings. τ is a temperature parameter used to adjust the scale.

In a batch, matched video and WiFi pairs are presented as positive examples, which can make the loss quite straightforward to fit. Therefore, for each video in a batch, we look for the most similar negative example among WiFi signals with different IDs, and similarly for WiFi signals, the function can be defined as follows:

$$\mathcal{L}_{dis} = \frac{1}{N} \sum_{i=1}^N [y_i \cdot D(v_i, w_i) + (1 - y_i) \cdot \max(0, (\text{margin} - D(v_i, w_i)))] \quad (5)$$

where v_i and w_i represent the feature embeddings of the video and WiFi signal, respectively, and y_i is the label of the corresponding index.

IV. EXPERIMENTS

A. Implementation Details

Our method is implemented within the PyTorch deep learning framework and trained on a single device equipped with a 4090 model GPU and 24G of VRAM. We use the Adam

TABLE I: Comparative experiment for the comparison with other person ReID methods from recent years.

Method	Publication	Input Modality	BackBone	Desc. Dim.	mAP	mINP	Rank-1	Rank-5	Rank-10
BoT [2]	CVPR	Vision	ResNet-50	2048	59.65	48.51	97.78	99.67	99.89
AGW [3]	TPAMI	Vision	ResNet-50	2048	66.12	35.90	97.02	99.27	99.60
SBS [4]	ArXiv	Vision	ResNet-50	2048	75.86	55.74	93.76	94.78	98.89
MGN [1]	ACM MM	Vision	ResNet-50	2048	71.71	42.42	99.49	99.89	99.93
SimpleViTfi [28]	IEICE	WiFi	ViT	768	70.73	47.08	92.73	99.09	99.09
ViFi-ReID(Only Vision)	----	Vision	ViViT	768	78.63	57.39	98.18	100.00	100.00
ViFi-ReID(Only Wi-Fi)	----	WiFi	WiFormer	768	75.49	59.67	91.82	98.18	99.09
ViFi-ReID(Full)	----	Vision+WiFi	ViViT+WiFormer	768	79.05	64.92	96.36	99.09	99.09

TABLE II: Ablation study for the retrieval task between vision and WiFi.

Method	WiFi-to-vision					vision-to-WiFi				
	mAP	mINP	Rank-1	Rank-5	Rank-10	mAP	mINP	Rank-1	Rank-5	Rank-10
Baseline	14.28	12.45	10.87	15.22	19.57	14.11	12.47	8.70	13.04	13.04
+VWC	77.61	66.62	78.26	94.57	98.91	75.01	66.09	76.09	91.30	95.65
+VWC+VWD	83.73	72.15	85.87	95.65	98.91	84.56	74.82	84.78	93.48	97.83

optimizer, spending 10 epochs to linearly increase the learning rate from 3.5×10^{-6} to 1×10^{-4} , then reduce the learning rate to 0.1 of its original at the 40-th and 90-th epochs, with the model being trained for a total of 120 epochs.

B. Comparison with State-of-the-Art methods

We conduct experiments on the ViFi-Indoors proposed in this letter, comparing our model with the state-of-the-art models. The results on the ViFi-Indoors test set for various models are displayed in Table I, which includes models with only visual information, only WiFi signals, and the full model utilizing both modalities of ViFi-ReID. It is evident that methods based purely on vision achieve higher Rank-N metrics. We observe that in purely visual approaches, the model is highly sensitive to RGB colors, which allows queries with a person's visual information to easily retrieve the same person's visual information with identical clothing in the gallery. However, visual information of the same person in different clothing receives lower similarity scores. Compared to other methods, our full model demonstrates superior performance in the mAP and mINP metrics, surpassing current single-modality ReID methods. Even when utilizing only one modality, our method remains competitive, and the full model exhibits higher robustness and accuracy, underscoring its effectiveness in the field of person ReID.

Figure 5 is shown that our method can significantly cluster the same pedestrian features in high-dimensional space, and the multimodal model can more accurately distinguish between positive and negative classes, exhibiting excellent recall and precision rates.

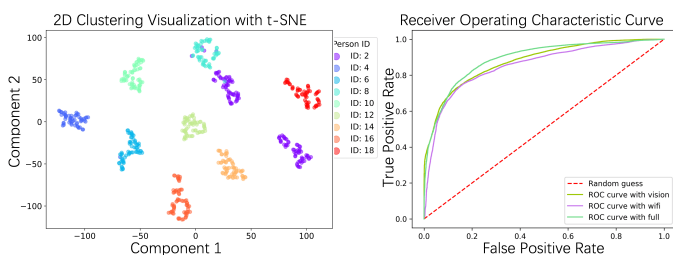


Fig. 5: Visualizations of pedestrian feature clustering in two-dimensional space and ROC curve.

C. Ablation study

The bottom three rows of Table I demonstrate that with the addition of modalities, ViFi-ReID's multimodal method indicates that vision and WiFi can complement each other with heterogeneous information, providing richer and more comprehensive expression of information than single-modality.

We use a baseline model that only undertakes ReID task learning without specifically learning the correspondence between vision and WiFi, and progressively incorporate our methods. As shown in Table II, our proposed approach significantly improves the precision and recall of cross-modal retrieval, achieving Rank-1 accuracies of 83.73% for WiFi-to-vision and 84.56% for vision-to-WiFi. This indicates that high-accuracy retrieval can be achieved between different modal data for the same person, significantly enhancing the perception range of ReID under different sensors.

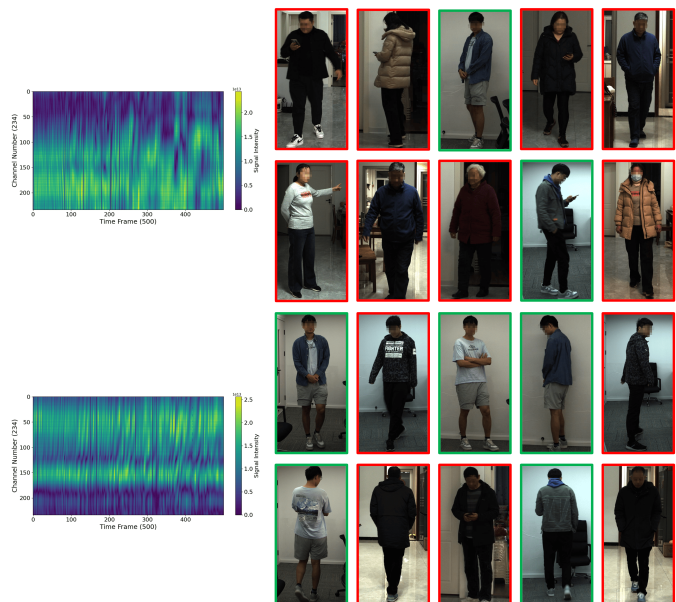


Fig. 6: Comparison of top-10 retrieved results on ViFi-Indoors between baseline (the first illustration) and our final method (the second illustration) for each WiFi query.

Figure 6 shows the top 10 retrieval results of the baseline and our final method, our method achieves more accurate retrieval results, matching and non-matching results marked with green and red rectangles, respectively.

V. CONCLUSION

We propose a person ReID method that utilizes both vision and WiFi, designed to address the limitations in robustness of single visual modal approaches and to expand the applicability of the task by bridging the gap between heterogeneous data types. According to our experimental results, ViFi-ReID outperforms other single-modal methods based on either WiFi or cameras. Additionally, it achieves impressive accuracy in vision-WiFi retrieval tasks, demonstrating that our method effectively bridges visual and signal modalities, making it suitable for more complex perception scenarios.

REFERENCES

- [1] G. Wang, Y. Yuan, X. Chen, J. Li, and X. Zhou, "Learning discriminative features with multiple granularities for person re-identification," in *Proceedings of the 26th ACM international conference on Multimedia*, 2018, pp. 274–282.
- [2] H. Luo, "Bags of tricks and a strong baseline for deep person re-identification," *IEEE*, 2019.
- [3] M. Ye, J. Shen, G. Lin, T. Xiang, L. Shao, and S. C. Hoi, "Deep learning for person re-identification: A survey and outlook," *IEEE transactions on pattern analysis and machine intelligence*, vol. 44, no. 6, pp. 2872–2893, 2021.
- [4] L. He, X. Liao, W. Liu, X. Liu, P. Cheng, and T. Mei, "Fastreid: A pytorch toolbox for real-world person re-identification," 2020.
- [5] X. Liu, P. Zhang, C. Yu, H. Lu, and X. Yang, "Watching you: Global-guided reciprocal learning for video-based person re-identification," 2021.
- [6] R. Hou, H. Chang, B. Ma, R. Huang, and S. Shan, "Bicnet-tks: Learning efficient spatial-temporal representation for video person re-identification," in *Proceedings of the IEEE/CVF conference on computer vision and pattern recognition*, 2021, pp. 2014–2023.
- [7] J. Liu, Z. J. Zha, W. Wu, K. Zheng, and Q. Sun, "Spatial-temporal correlation and topology learning for person re-identification in videos," 2021.
- [8] S. Li, L. Sun, and Q. Li, "Clip-reid: exploiting vision-language model for image re-identification without concrete text labels," in *Proceedings of the AAAI Conference on Artificial Intelligence*, vol. 37, no. 1, 2023, pp. 1405–1413.
- [9] Z. Sun and F. Zhao, "Counterfactual attention alignment for visible-infrared cross-modality person re-identification," *Pattern recognition letters*, 2023.
- [10] Z. Wu and M. Ye, "Unsupervised visible-infrared person re-identification via progressive graph matching and alternate learning," in *Proceedings of the IEEE/CVF Conference on Computer Vision and Pattern Recognition*, 2023, pp. 9548–9558.
- [11] Y. Zhang and H. Wang, "Diverse embedding expansion network and low-light cross-modality benchmark for visible-infrared person re-identification," in *Proceedings of the IEEE/CVF Conference on Computer Vision and Pattern Recognition*, 2023, pp. 2153–2162.
- [12] B. Li, W. Cui, W. Wang, L. Zhang, Z. Chen, and M. Wu, "Two-stream convolution augmented transformer for human activity recognition," in *Proceedings of the AAAI Conference on Artificial Intelligence*, vol. 35, no. 1, 2021, pp. 286–293.
- [13] Y. Zhou, C. Xu, L. Zhao, A. Zhu, F. Hu, and Y. Li, "Csi-former: Pay more attention to pose estimation with wifi," *Entropy*, vol. 25, no. 1, p. 20, 2022.
- [14] M. Zhao, T. Li, M. A. Alsheikh, Y. Tian, and D. Katabi, "Through-wall human pose estimation using radio signals," in *Computer Vision and Pattern Recognition (CVPR)*, 2018.
- [15] Z. Zhang, H. Du, S. Choi, and S. H. Cho, "Tips: Transformer based indoor positioning system using both csi and doa of wifi signal," *IEEE Access*, vol. 10, pp. 111 363–111 376, 2022.
- [16] X. Wang, L. Gao, and S. Mao, *PhaseFi: Phase Fingerprinting for Indoor Localization with a Deep Learning Approach*. PhaseFi: Phase Fingerprinting for Indoor Localization with a Deep Learning Approach., 2015.
- [17] D. Avola, M. Cascio, L. Cinque, and D. Pannone, "Wi-fi passive person re-identification based on channel state information," 2019.
- [18] Y. Liu, W. Zhou, M. Xi, S. Shen, and H. Li, "Multi-modal context propagation for person re-identification with wireless positioning," *IEEE Transactions on Multimedia*, vol. PP, no. 99, pp. 1–1, 2021.
- [19] D. Avola, M. Cascio, L. Cinque, A. Fagioli, and C. Petrioli, "Person re-identification through wi-fi extracted radio biometric signatures," *IEEE Transactions on Information Forensics and Security*, vol. 17, pp. 1145–1158, 2022.
- [20] Y. Liu, W. Zhou, M. Xi, S. Shen, and H. Li, "Vision meets wireless positioning: Effective person re-identification with recurrent context propagation," 2020.
- [21] L. Deng, J. Yang, S. Yuan, H. Zou, C. X. Lu, and L. Xie, "Gaitfi: Robust device-free human identification via wifi and vision multimodal learning," *IEEE Internet of Things Journal*, vol. 10, no. 1, pp. 625–636, 2022.
- [22] B. Korany, C. R. Karanam, H. Cai, and Y. Mostofi, "Xmodal-id: Using wifi for through-wall person identification from candidate video footage," 2019.
- [23] C. Mao, C. Tan, J. Hu, and M. Zheng, "Time-frequency analysis of variable-length wifi csi signals for person re-identification," *IEEE Signal Processing Letters*, pp. 1–5, 2024.
- [24] A. Vaswani, N. Shazeer, N. Parmar, J. Uszkoreit, L. Jones, A. N. Gomez, Ł. Kaiser, and I. Polosukhin, "Attention is all you need," *Advances in neural information processing systems*, vol. 30, 2017.
- [25] A. Arnab, M. Dehghani, G. Heigold, C. Sun, M. Lučić, and C. Schmid, "Vivit: A video vision transformer," in *Proceedings of the IEEE/CVF international conference on computer vision*, 2021, pp. 6836–6846.
- [26] J. Devlin, M. W. Chang, K. Lee, and K. Toutanova, "Bert: Pre-training of deep bidirectional transformers for language understanding," 2018.
- [27] Z. Y. Dou, Y. Xu, Z. Gan, J. Wang, S. Wang, L. Wang, C. Zhu, P. Zhang, L. Yuan, and N. Peng, "An empirical study of training end-to-end vision-and-language transformers," 2021.
- [28] J. Bian, M. Zheng, H. Liu, J. Mao, H. Li, and C. Tan, "Simplevitfi: A lightweight vision transformer model for wi-fi-based person identification," *IEICE Transactions on Communications*, vol. E107-B, no. 4, 2024.
- [29] H. Wang, Y. Wang, Z. Zhou, X. Ji, D. Gong, J. Zhou, Z. Li, and W. Liu, "Cosface: Large margin cosine loss for deep face recognition," *IEEE*, 2018.
- [30] Q. Qian, L. Shang, B. Sun, J. Hu, H. Li, and R. Jin, "Softtriple loss: Deep metric learning without triplet sampling," in *arXiv*, 2019.
- [31] A. Radford, J. W. Kim, C. Hallacy, A. Ramesh, G. Goh, S. Agarwal, G. Sastry, A. Askell, P. Mishkin, and J. Clark, "Learning transferable visual models from natural language supervision," 2021.
- [32] P. Khosla, P. Teterwak, C. Wang, A. Sarna, Y. Tian, P. Isola, A. Maschinot, C. Liu, and D. Krishnan, "Supervised contrastive learning," 2020.